



Institute of  
Space Sciences  
CSIC  
IEEC<sup>9</sup>

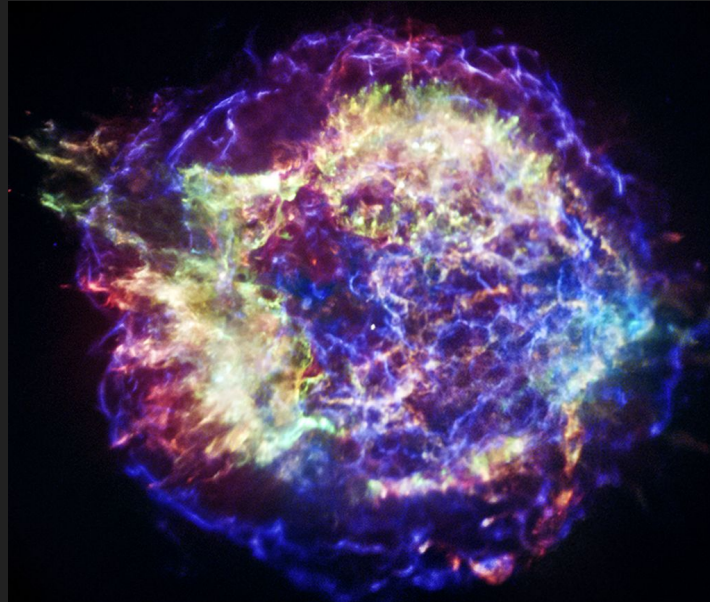


University of Hertfordshire,  
November 21th 2023

# Simulation-based inference (sbi) for pulsar population synthesis

Dr. Vanessa Gruber ([gruber@ice.csic.es](mailto:gruber@ice.csic.es))

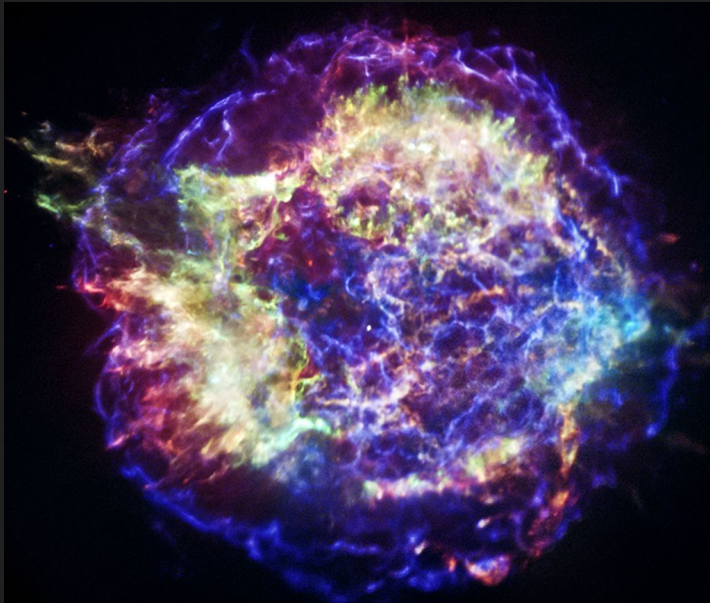
in collaboration with Michele Ronchi,  
Celsa Pardo Araujo, and Nanda Rea



Cassiopeia A supernova remnant  
(credit: NASA/CXC/SAO)

# Outline

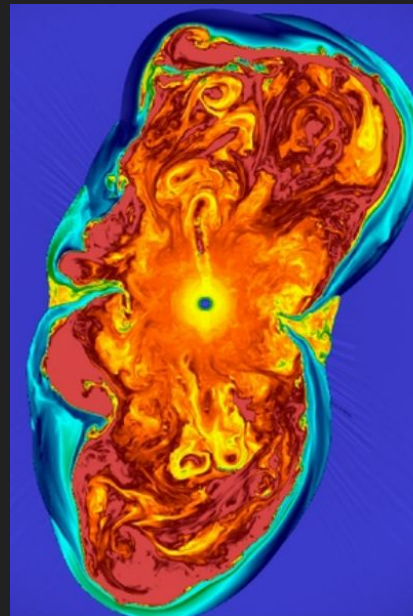
- **Neutron stars**
- **Pulsar population synthesis**
- **Machine learning and sbi**
- **Inference results**
- **Outlook**



Cassiopeia A supernova remnant  
(credit: NASA/CXC/SAO)

# Neutron-star formation

- Neutron stars are one of three types of **compact remnants**, created during the **final stages of stellar evolution**.
- When a **massive star of 8 - 25 solar masses** runs out of fuel, it collapses under its own gravitational attraction and **explodes in a supernova**.
- During the collapse, **electron capture** processes ( $p + e^- \rightarrow n + \nu_e$ ) produce (a lot of) neutrons.



**mass:**  $1.2 - 2.1 M_{\odot}$

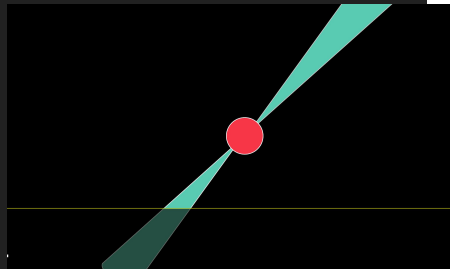
**radius:** 9 - 15 km

**density:**  $10^{15} g/cm^3$

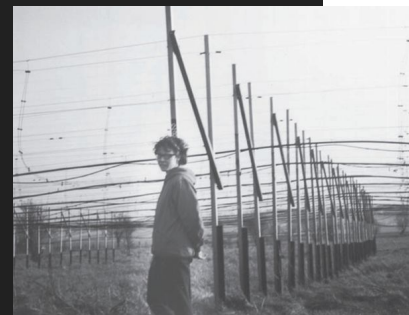
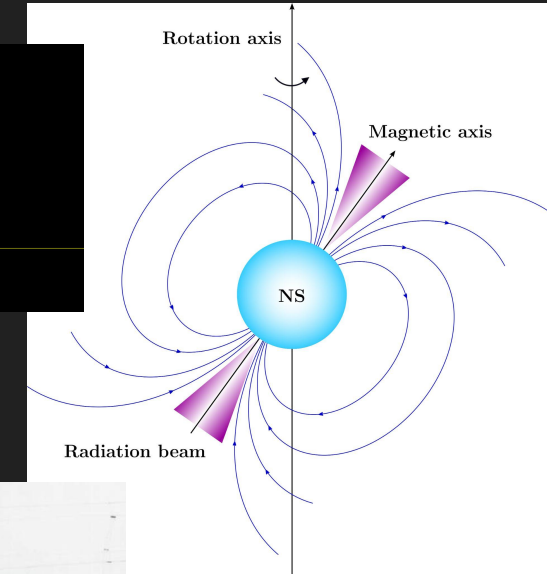
Snapshot of a 3D core-collapse supernova simulation (Mösta et al., 2014)

# Lighthouse radiation

- Neutron stars have **extreme magnetic fields** between  $10^8$  -  $10^{15}$  G. For comparison, the Earth's magnetic field is 0.5 G.
- Because rotation and magnetic axes are misaligned, neutron stars emit radio beams **like a lighthouse**.
- These pulses can be observed with radio telescopes. This is how neutron stars were first detected and why we call them **pulsars**.



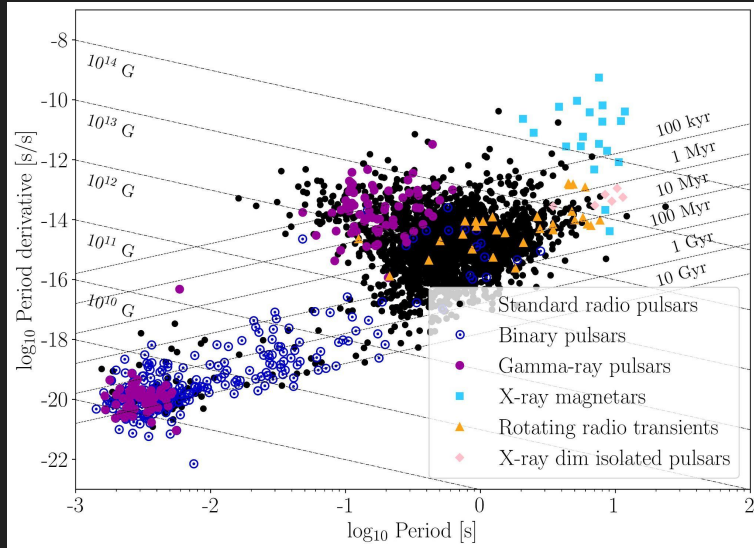
Credit: J. Christiansen



Sketch of the neutron-star exterior.

Dame Jocelyn Bell Burnell in front of her radio telescope in Cambridge, UK.

# The neutron-star zoo



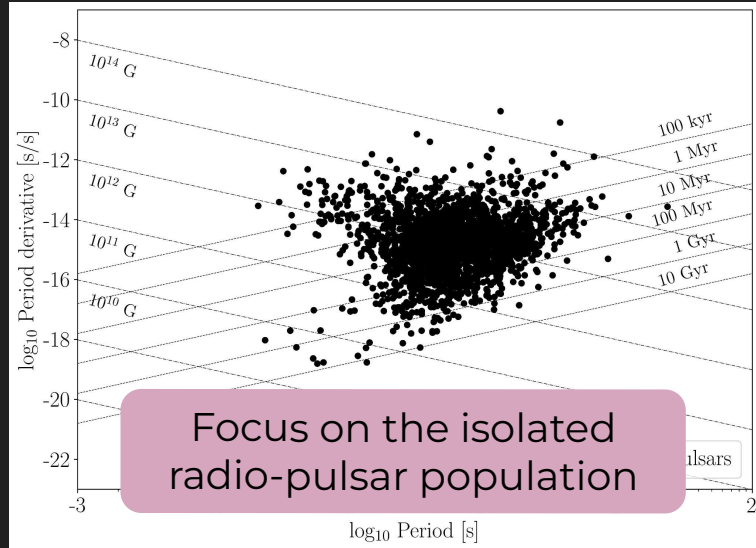
Period period-derivative plane for the pulsar population. Data taken from the ATNF Pulsar Catalogue (Manchester et al., 2005)

- Pulsars are **very precise clocks** and we time their pulses to **measure rotation periods  $P$  and derivatives  $\dot{P}$** .
- We now observe neutron stars as pulsars **across the electromagnetic spectrum**.

~ **3,000 pulsars** are known to date

- Grouping neutron stars in the  **$P\dot{P}$ -plane** according to their observed properties serves as a diagnostic tool to **identify different neutron-star classes**.

# The neutron-star zoo



Period period-derivative plane for the pulsar population. Data taken from the ATNF Pulsar Catalogue (Manchester et al., 2005)

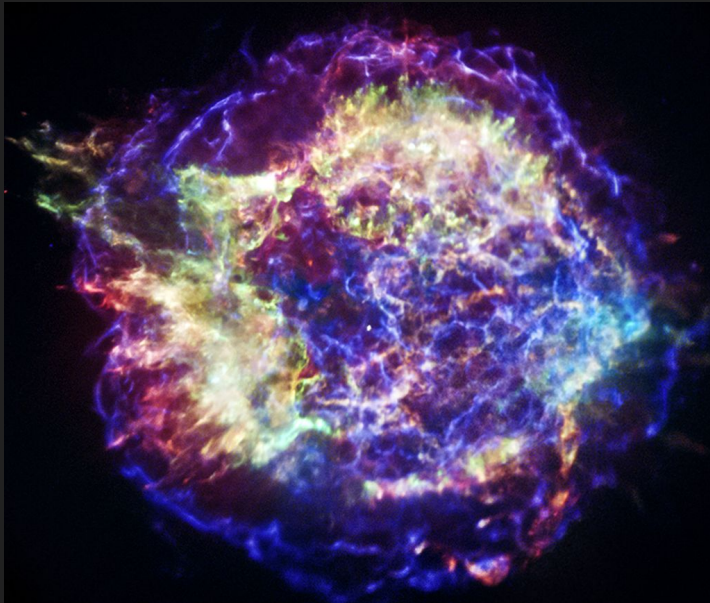
- Pulsars are **very precise clocks** and we time their pulses to **measure rotation periods  $P$  and derivatives  $\dot{P}$** .
- We now observe neutron stars as pulsars **across the electromagnetic spectrum**.

~ 3,000 pulsars are known to date

- Grouping neutron stars in the  **$P\dot{P}$ -plane** according to their observed properties serves as a diagnostic tool to **identify different neutron-star classes**.

# Outline

- **Neutron stars**
- **Pulsar population synthesis**
- **Machine learning and sbi**
- **Inference results**
- **Outlook**



Cassiopeia A supernova remnant  
(credit: NASA/CXC/SAO)

# General idea

- We can estimate the **total number of neutron stars in our Galaxy**

$$\text{CC supernova rate: } \sim 2 \text{ per century} \times \text{Galaxy age: } \sim 13.6 \text{ billion years} = \text{NS number: } \sim 2.8 \times 10^8$$

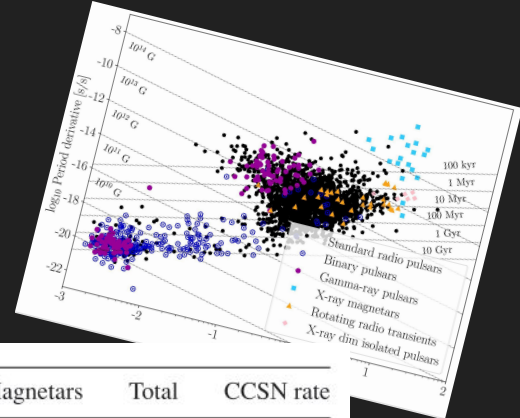
- We only **detect** a very **small fraction** of all neutron stars. Population synthesis bridges this gap focusing on the full population of neutron stars (e.g. Faucher-Giguère & Kaspi 2006, Lorimer et al. 2006, Gullón et al. 2014, Cieślar et al. 2020):



# Goals

- Population synthesis allows us to **constrain the natal properties** of neutron stars and their **birth rates**.
- This is for example **relevant for**:
  - Massive star evolution
  - Gamma-ray bursts
  - Fast-radio bursts
  - Peculiar supernovae
- We can also learn about **evolutionary links between different neutron-star classes** (e.g., Viganó et al., 2013). This is important because estimates for the **Galactic core-collapse supernova rate** are **insufficient** for to explain the independent formation of different classes of pulsars (Keane & Kramer, 2008).

Estimated Galactic core-collapse supernova rate and birth rates for different pulsar classes (Keane & Kramer, 2008).



PSRs	RRATs	XDINSS	Magnetars	Total	CCSN rate
$2.8 \pm 0.5$	$5.6^{+4.3}_{-3.3}$	$2.1 \pm 1.0$	$0.3^{+1.2}_{-0.2}$	$10.8^{+7.0}_{-5.0}$	$1.9 \pm 1.1$
$1.4 \pm 0.2$	$2.8^{+1.6}_{-1.6}$	$2.1 \pm 1.0$	$0.3^{+1.2}_{-0.2}$	$6.6^{+4.0}_{-3.0}$	$1.9 \pm 1.1$
$1.1 \pm 0.2$	$2.2^{+1.7}_{-1.3}$	$2.1 \pm 1.0$	$0.3^{+1.2}_{-0.2}$	$5.7^{+4.1}_{-2.7}$	$1.9 \pm 1.1$
$1.6 \pm 0.3$	$3.2^{+2.5}_{-1.9}$	$2.1 \pm 1.0$	$0.3^{+1.2}_{-0.2}$	$7.2^{+5.0}_{-3.4}$	$1.9 \pm 1.1$
$1.1 \pm 0.2$	$2.2^{+1.7}_{-1.3}$	$2.1 \pm 1.0$	$0.3^{+1.2}_{-0.2}$	$5.7^{+4.1}_{-2.7}$	$1.9 \pm 1.1$

# Dynamical evolution I

- **Neutron stars are born in star-forming regions**, i.e., in the Galactic disk along the Milky Way's spiral arms, **and receive kicks** during the supernova explosions.
- We make the following assumptions:
  - Spiral-arm model (Yao et al., 2017) plus rigid rotation with  $T = 250$  Myr
  - **Exponential disk model** with scale height  $h_c$  (Wainscoat et al., 1992)
  - Single-component **Maxwell kick-velocity distribution** with dispersion  $\sigma_k$  (Hobbs et al., 2005)
  - Galactic potential (Marchetti et al., 2019)

Artistic illustration of the Milky Way (credit: NASA JPL)



$$\mathcal{P}(z) = \frac{1}{h_c} e^{-\frac{|z|}{h_c}}$$

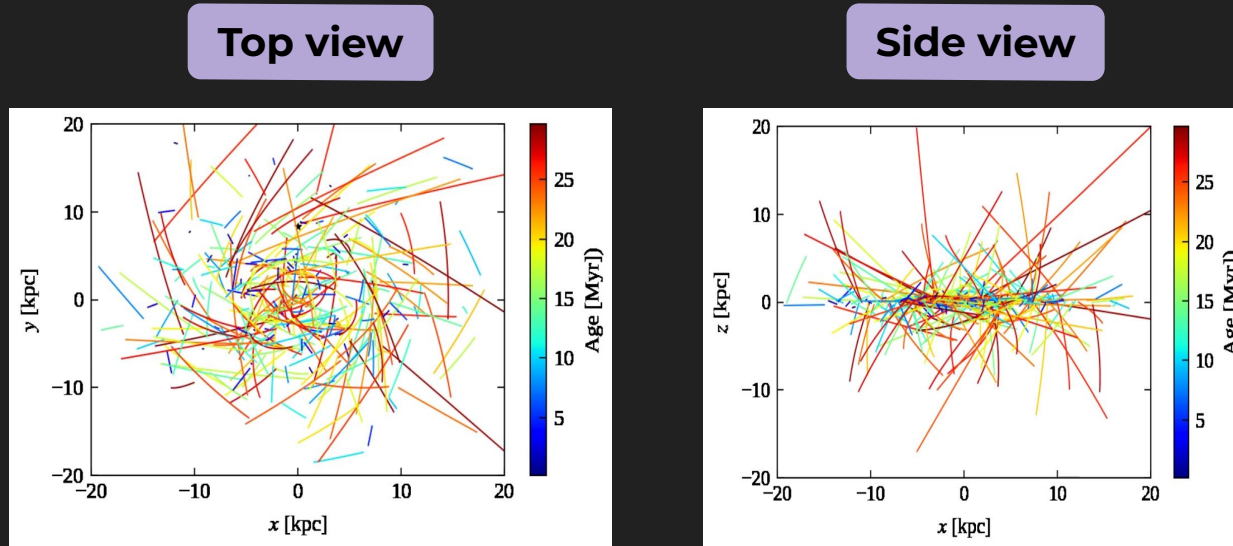
$$\mathcal{P}(v_k) = \sqrt{\frac{2}{\pi}} \frac{v_k^2}{\sigma_k^3} e^{-\frac{v_k^2}{2\sigma_k^2}}$$

For Monte-Carlo approach,  
we **vary two uncertain parameters  $h_c$  and  $\sigma_k$** .

# Dynamical evolution II

- For our Galactic model  $\Phi_{\text{MW}}$ , we evolve the stars' position & velocity by **solving Newtonian equations of motion** in cylindrical galactocentric coordinates:

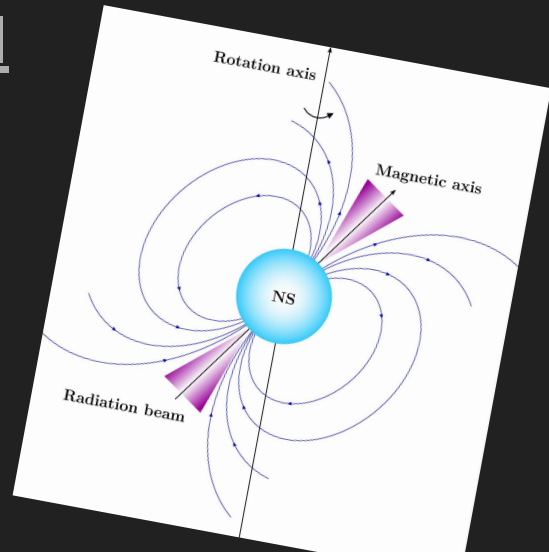
$$\ddot{\vec{r}} = -\vec{\nabla}\Phi_{\text{MW}}$$



Galactic evolution tracks for  $h_c = 0.18$  kpc,  $\sigma = 265$  km/s.

# Magneto-rotational evolution I

- The neutron-star magnetosphere exerts a **torque onto the star**. This causes **spin-down** and **alignment of the magnetic and rotation axes**.
- Neutron star **magnetic fields decay** due to the Hall effect and Ohmic dissipation in the outer stellar layer (crust) (e.g., Viganó et al., 2013 & 2021).
- We make the following assumptions:
  - **Initial periods** follow a log-normal with  $\mu_P$  and  $\sigma_P$  (Igoshev et al., 2022)
  - **Initial fields** follow a log-normal with  $\mu_B$  and  $\sigma_B$  (Gullón et al., 2014)
  - Above  $T \sim 10^6$  yr, **field decay** follows a power-law with  $B(t) \sim B_0 (1 + t/T)^\alpha$ .



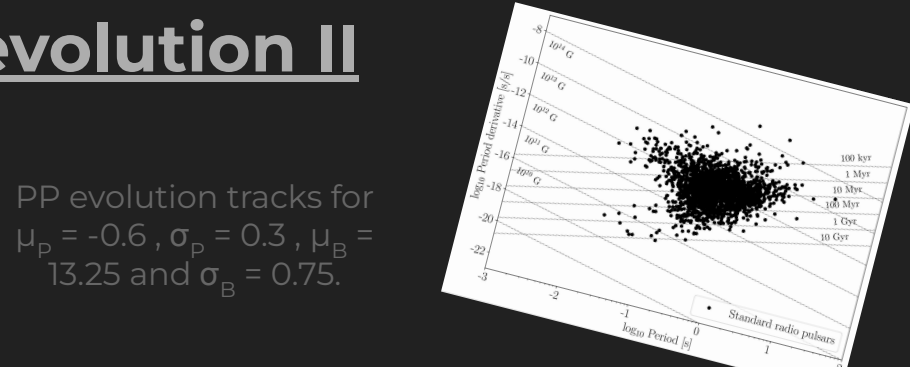
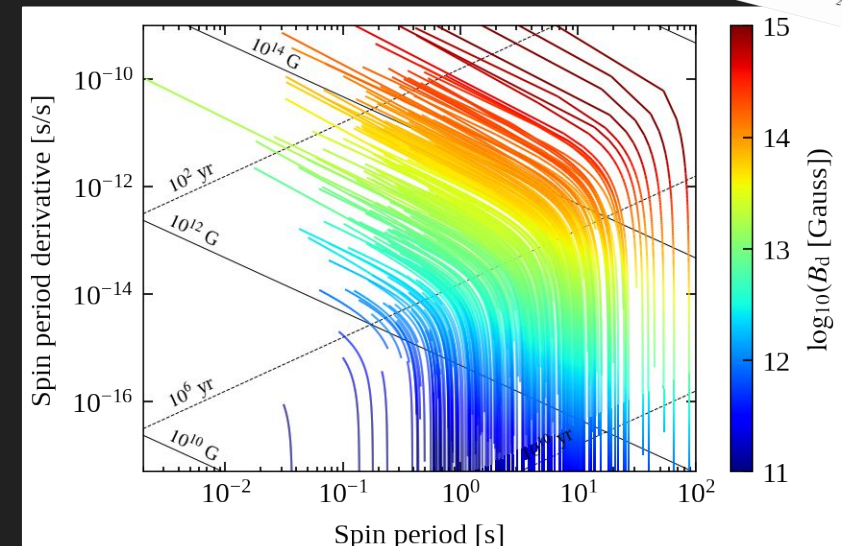
$$\mathcal{P}(\log P_0) = \frac{1}{\sqrt{2\pi}\sigma_P} \exp\left(-\frac{[\log P_0 - \mu_P]^2}{2\sigma_P^2}\right)$$

Here, we **vary** the five uncertain parameters  $\mu_P$ ,  $\mu_B$ ,  $\sigma_P$ ,  $\sigma_B$  and  $\alpha$ .

# Magneto-rotational evolution II

- To model the magneto-rotational evolution, we numerically **solve two coupled ordinary differential equations** for the period and the misalignment angle (Aguilera et al., 2008; Philippov et al. 2014).
- We use results from **2D magneto-thermal simulations** to determine the evolution of the magnetic field.
- This allows us to follow the stars'  $P$  and  $\dot{P}$  evolution in the PP-plane.

PP evolution tracks for  $\mu_P = -0.6$ ,  $\sigma_P = 0.3$ ,  $\mu_B = 13.25$  and  $\sigma_B = 0.75$ .



# Radio emission and detection

- The stars' **rotational energy  $E_{\text{rot}}$**  is converted into coherent radio emission. We assume that the corresponding **radio luminosity  $L_{\text{radio}}$**  is proportional to the loss of  $E_{\text{rot}}$  (Faucher- Giguère & Kaspi, 2006; Gullón et al., 2014).  $L_0$  is taken from observations.
- As **emission is beamed**, ~ 90% of pulsars do not point towards us. For those intercepting our line of sight, compute **radio flux  $S_{\text{radio}}$**  & **pulse width  $W$** .

$$L_{\text{radio}} = L_0 \left( \frac{\dot{P}}{P^3} \right)^{1/2} \propto \dot{E}_{\text{dot}}^{1/2}$$

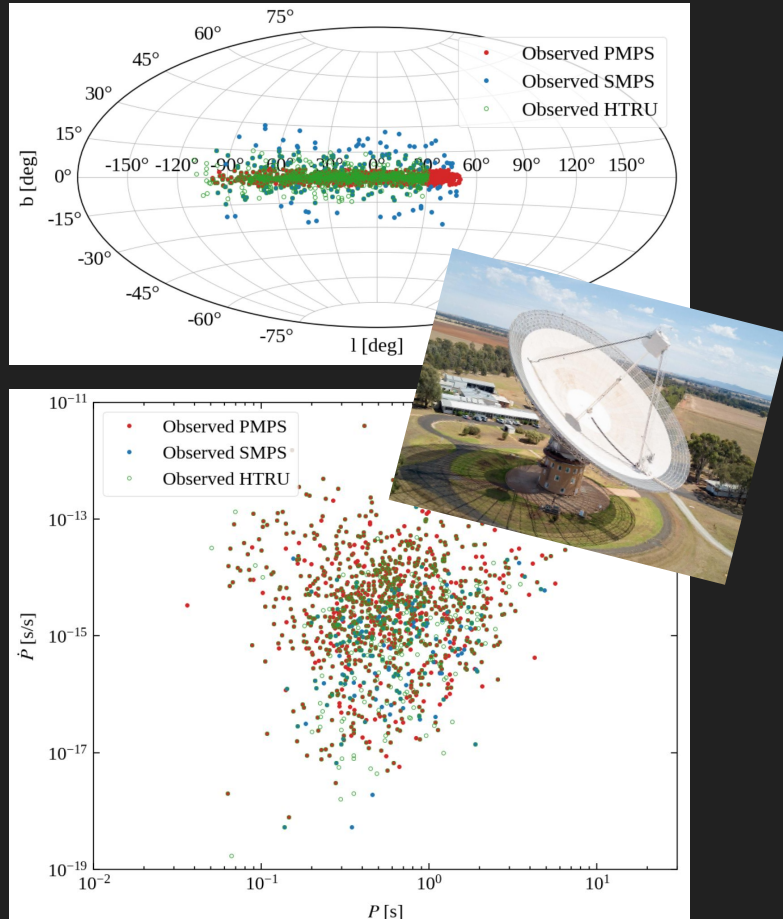
$$S_{\text{radio}} = \frac{L_{\text{radio}}}{\Omega_{\text{beam}} d^2}$$

A pulsar counts as detected, if it **exceeds the sensitivity threshold** for a survey recorded with a specific radio telescope.

# Three pulsar surveys

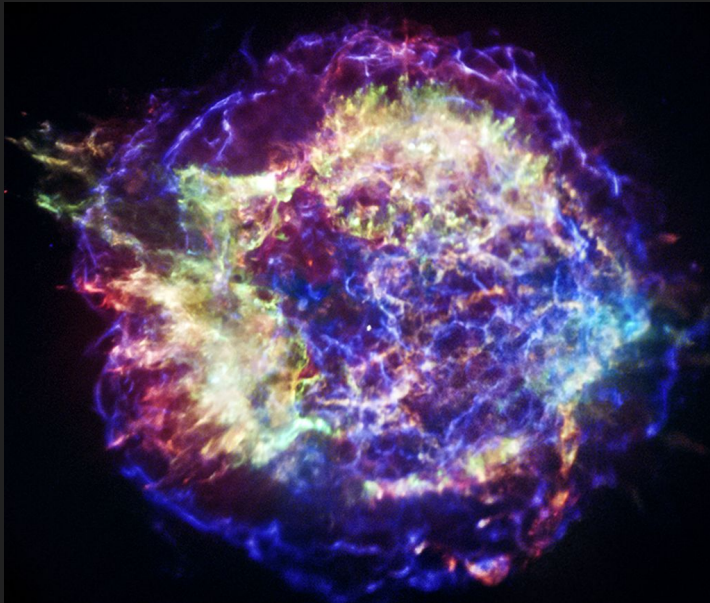
- We compare our simulated populations with three surveys from Murriyang (the Parkes Radio Telescope):
  - **Parkes Multibeam Pulsar Survey** (PMPS): 1,009 *isolated pulsars*
  - **Swinburne Parkes Multibeam Pulsar Survey** (SMPS): 218 *isol. p.*
  - **High Time Resolution Universe Survey** (HTRU): 1,023 *isol. pulsars*

**Can we constrain birth properties by looking at a current snapshot of the pulsar population?**



# Outline

- **Neutron stars**
- **Pulsar population synthesis**
- **Machine learning and sbi**
- **Inference results**
- **Outlook**



Cassiopeia A supernova remnant  
(credit: NASA/CXC/SAO)



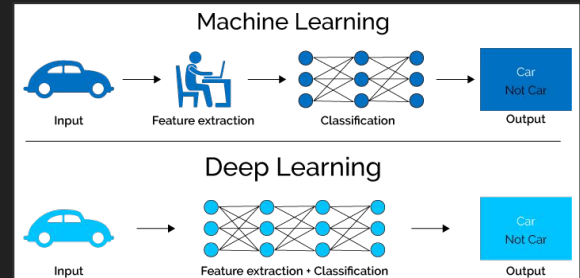
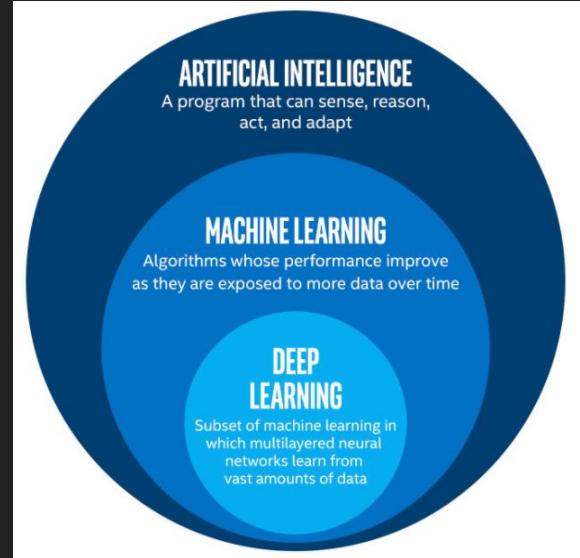
## Comparing models and data

- Comparing observations to models and **constraining regions of the parameter space** that are **most probable given the data** is fundamental to many fields of science.
- Pulsar population synthesis is complex and has **many free parameters**. To compare synthetic simulations with observations, people have
  - Randomly sampled and then optimised ‘by eye’ (e.g., Gonthier et al., 2007)
  - Compared distributions of individual parameters using  $\chi^2$ - and KS-tests (e.g., Narayan & Ostriker, 1990; Faucher-Giguère & Kaspi, 2006)
  - Used annealing methods for optimisation (Gullón et al., 2014)
  - Performed Bayesian inference for simplified models (Cieślar et al., 2020)

These methods do not scale well and are **difficult to use** with the **multi-dimensional data** produced in population synthesis.

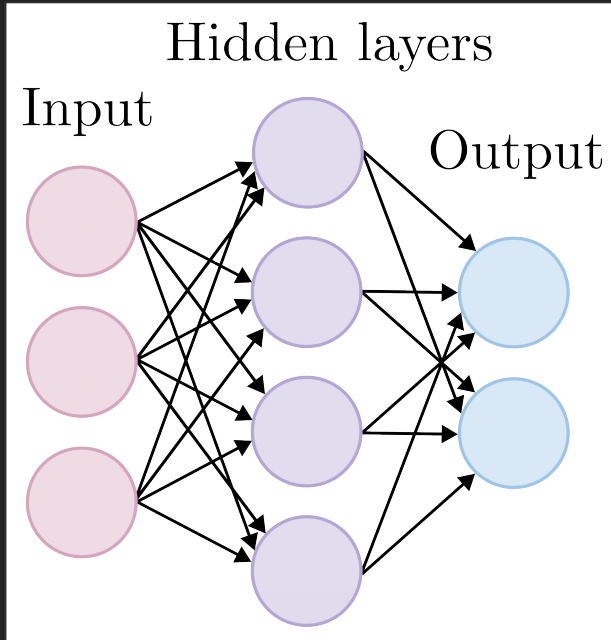
# Deep learning

- Deep Learning is a subfield of Artificial Intelligence and Machine Learning. It focuses on using **multi-layered neural networks** to learn from large datasets. Different to classical ML approaches, deep learning does **not require external feature engineering**.
- **Recognising features in a hierarchical way** allows deep neural networks to model **complex non-linear relationships** for large input data. This makes deep learning powerful when **working with unstructured data such as images**, where the number of features / pixel can easily exceed millions.



Credit: [www.bigdata-insider.de](http://www.bigdata-insider.de) (top), Acheron Analytics (bottom)

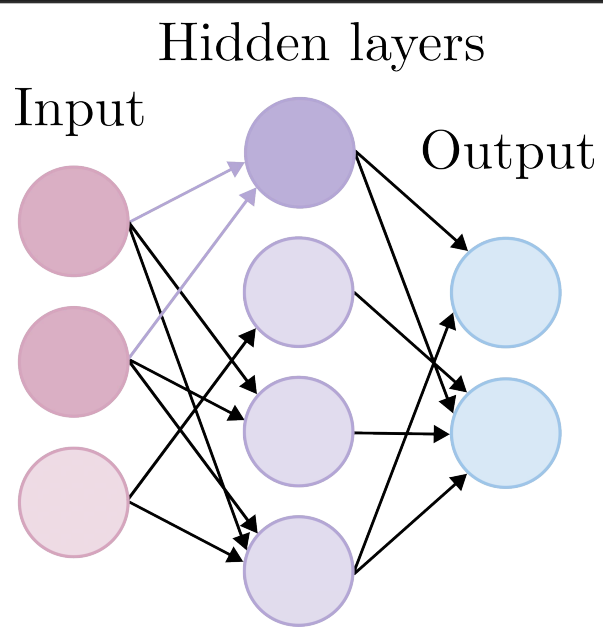
# Convolutional neural networks (CNNs)



Sketch of a very simple  
fully connected neural network.

- A neural network is composed of layers, which represent **stacks of neurons** (objects holding a single numerical value). Each layer encodes a simplified representation of the input data.
- A deep-learning **algorithm learns more and more about the input** as the data is passed through successive network layers.
- The **Multilayer Perceptron** is the simplest set-up where input and output are **fully connected**. In a CNN, not all nodes are connected, which **reduces the number of trainable parameters** and allows more flexibility for training.

# Convolutional neural networks (CNNs)



Sketch of a very simple convolutional neural network.

- A neural network is composed of layers, which represent **stacks of neurons** (objects holding a single numerical value). Each layer encodes a simplified representation of the input data.
- A deep-learning **algorithm learns more and more about the input** as the data is passed through successive network layers.
- The **Multilayer Perceptron** is the simplest set-up where input and output are **fully connected**. In a CNN, not all nodes are connected, which **reduces the number of trainable parameters** and allows more flexibility for training.

# Convolutional and max pooling layers

- Besides fully connected layers, CNNs are composed of two types of filters:

## Convolutional filters



$$\begin{bmatrix} -1 & -1 & -1 \\ -1 & 8 & -1 \\ -1 & -1 & -1 \end{bmatrix}$$



## Max-pooling layers

3	1	0	9
8	4	7	3
6	5	0	4
1	2	9	0

$2 \times 2$

8	9
6	9

These filters recognise features, such as detecting edges of an object in an image.

These filters extract the most relevant features, helping to speed up the training process.

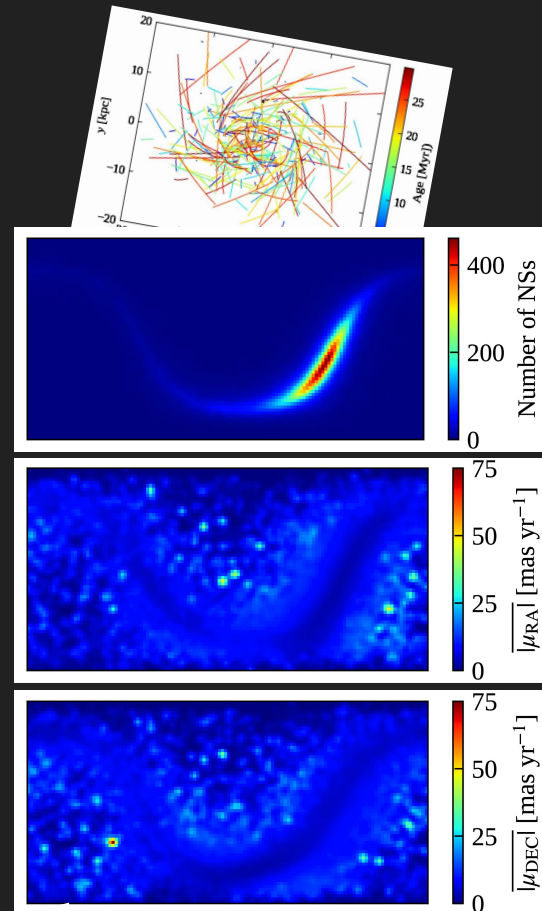
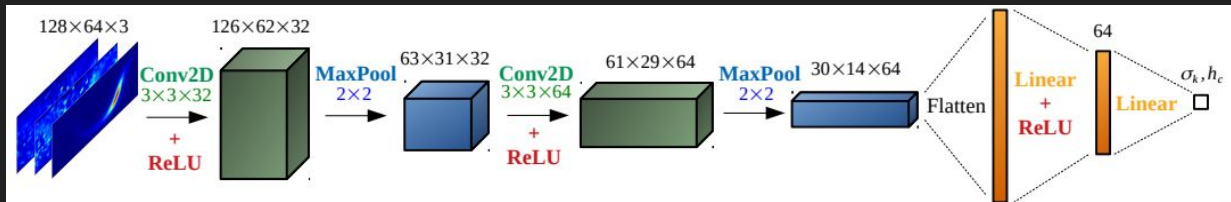
# Proof of concept study I

- In Ronchi et al. (2021), we focused on the dynamical evolution and **simulated a database of 128 x 128 (=16,384) synthetic neutron-star populations.**

Vary **scale height**  
 $h_c$  in range  
[0.02-2] kpc

Vary **dispersion**  $\sigma_k$  of  
kick distribution  
between [1-700] km/s

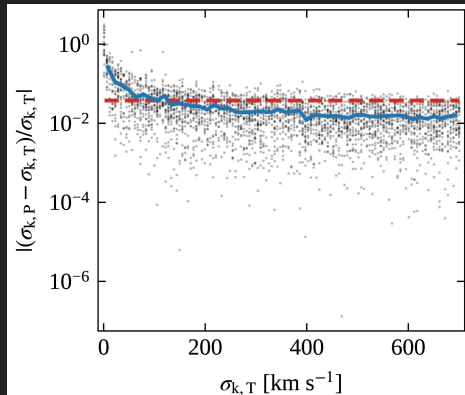
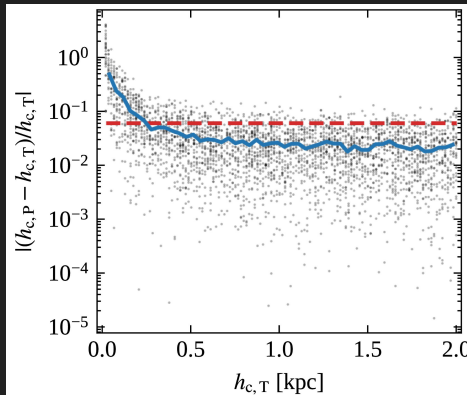
- We **perform supervised ML** and train a CNN to extract labels  $h_c$  and  $\sigma$  from position / velocity maps:



Stellar density and velocity maps in ICRS coordinates.

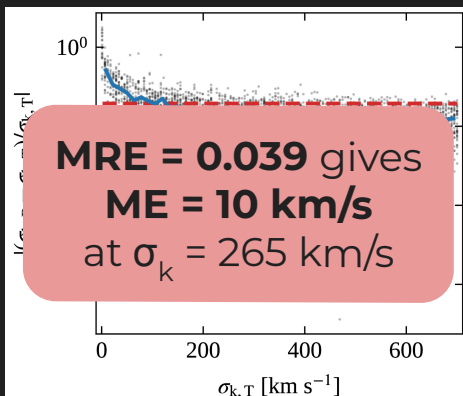
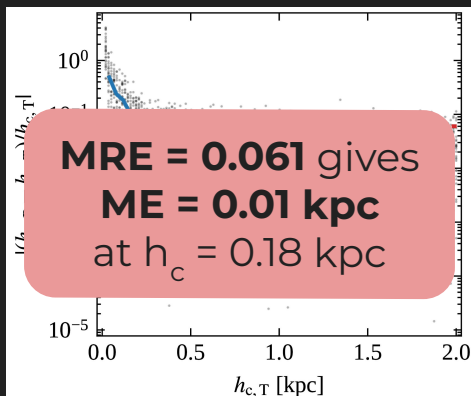
# Proof of concept study II

- **Training info:** We use the root mean square error as the loss function and validation metric, Kaiming initialisation, Adam for gradient-descent optimisation, and apply a 80 / 20% split of the full dataset for training and validation.
- The **CNN recovers the input values** very well. To visualise this, we can look at the **relative error between target and predicted labels**



# Proof of concept study II

- **Training info:** We use the root mean square error as the loss function and validation metric, Kaiming initialisation, Adam for gradient-descent optimisation, and apply a 80 / 20% split of the full dataset for training and validation.
- The **CNN recovers the input values** very well. To visualise this, we can look at the **relative error between target and predicted labels**



We did **not include observational biases** and assumed all simulated stars are detectable! **216 pulsars have measured proper motions**, insufficient for this precision.

# Statistical inference

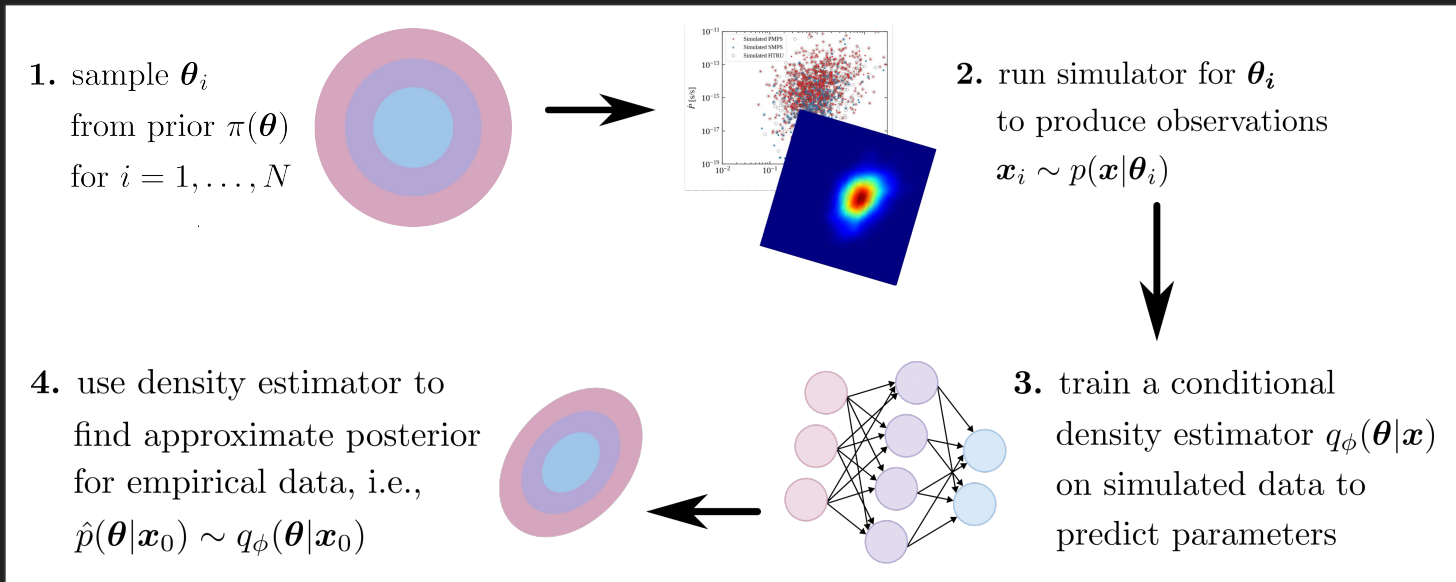
- Our initial study focused on **deducing point estimates**. However, we often do not require exact estimates but **knowledge of probable regions** is sufficient.
- This is where **Bayesian inference** comes in: based on some prior knowledge  $\pi(\theta)$ , a stochastic model and some observation  $x$ , we want to infer the most likely distribution  $P(\theta|x)$  for our model parameters  $\theta$  given the data  $x$ . This is **encoded in Bayes' Theorem**:

$$\underbrace{P(\theta|x)}_{\text{posterior}} = \frac{\overbrace{P(\theta)}^{\text{prior } \pi} \overbrace{P(x|\theta)}^{\text{likelihood } \mathcal{L}}}{\underbrace{P(x)}_{\text{evidence}}} = \frac{P(\theta) \int P(x,z|\theta) dz}{\int P(x|\theta') P(\theta') d\theta'}$$

For complex simulators, the **likelihood is defined implicitly and often intractable**. This is overcome with **simulation-based** (likelihood-free) **inference** (see e.g. Cranmer et al., 2020).

# Simulation-based inference I

- To perform **Bayesian inference for any kind of (stochastic) forward model** (e.g. those specified by simulators), we use the following approach:



# Simulation-based inference II

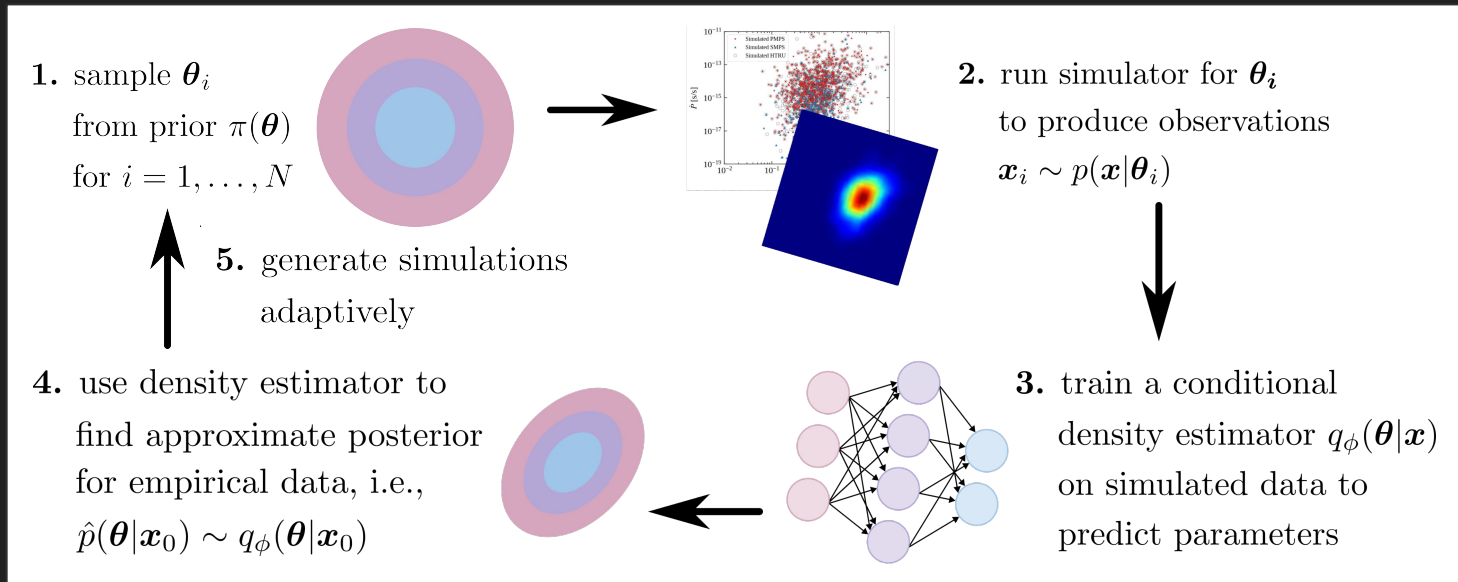
- Different approaches (all relying on deep learning) exist to **learn a probabilistic association** between the simulated data and the underlying parameters. These algorithms essentially focus on different pieces of Bayes' theorem:
  - Neural Posterior Estimation (NPE) (e.g., Papamakarios & Murray, 2016)
  - Neural Likelihood Estimation (NLE) (e.g., Papamakarios et al., 2019)
  - Neural Ratio Estimation (NRE) (e.g., Hermans et al., 2020; Delaunoy et al., 2022)

**We focus on NPE.** This allows us to **directly learn the posterior distribution**. In contrast, NLE and NRE need an extra (potentially time consuming) MCMC sampling step to construct a posterior.

- All methods exist in **sequential form** (SNPE, SNLE, SNRE), **which adds a fifth step to workflow**. Instead of sampling from the prior, we adaptively generate simulations from the posterior. This **typically requires fewer simulations**.

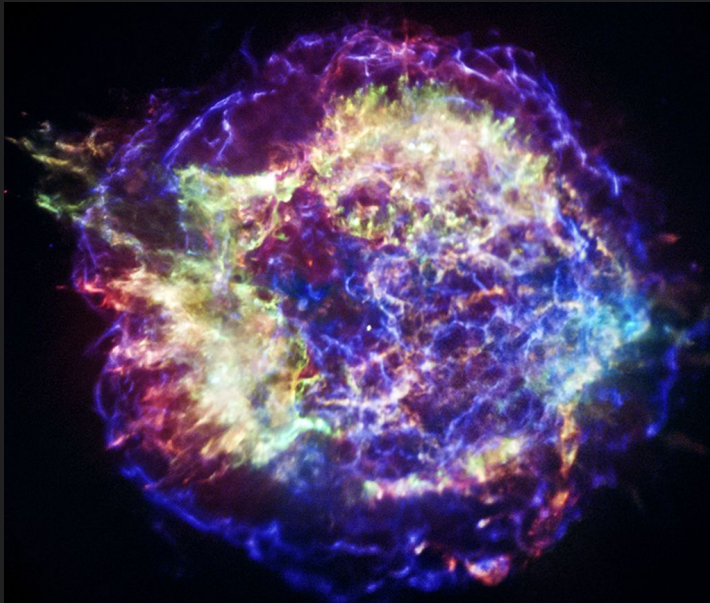
# Simulation-based inference I

- To perform **Bayesian inference for any kind of (stochastic) forward model** (e.g. those specified by simulators), we use the following approach:



# Outline

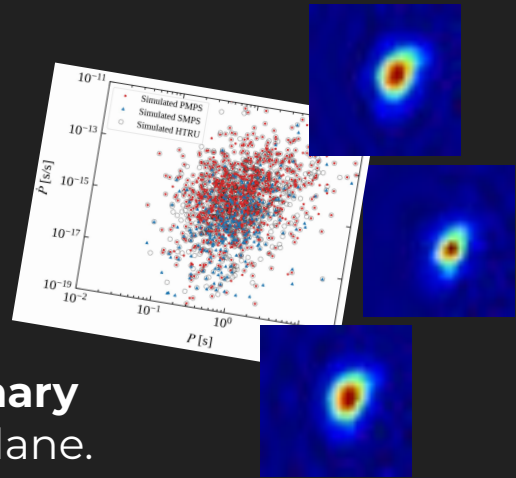
- **Neutron stars**
- **Pulsar population synthesis**
- **Machine learning and sbi**
- **Inference results**
- **Outlook**



Cassiopeia A supernova remnant  
(credit: NASA/CXC/SAO)

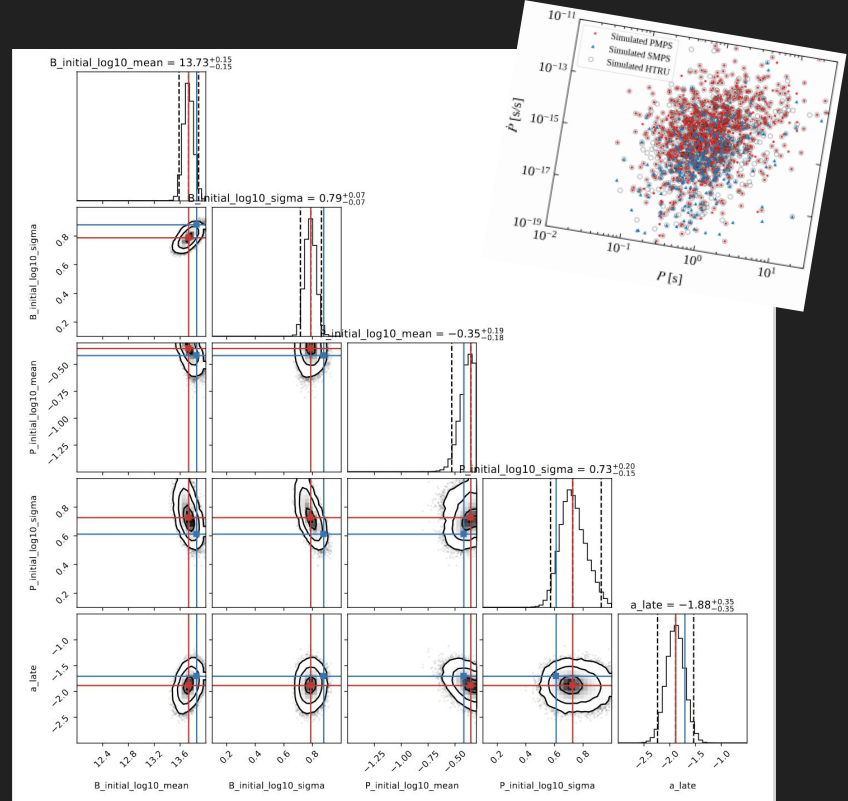
# Workflow

- With our complex population synthesis simulator, we fix the dynamics to a fiducial model and **focus on the magneto-rotational evolution**.
- From our simulated populations, we **generate summary statistics**: density maps for three surveys in the PP-plane.
- To perform the inference, we use the **PyTorch package sbi** (Tejero-Cantero et al., 2020; <https://www.mackelab.org/sbi/>). Our trainable neural network has two parts:
  - CNN** (see Ronchi et al., 2021): compresses the data into a latent vector.
  - Mixture density network**: our posterior is approximated by a mixture of 10 Gaussians components; we learn the means, stds and coefficients.
- We initialise the CNN with Kaiming, use 89% of data for training, 10% for validation and 1% for testing, set the batch size to 8, and learning rate to  $5 \times 10^{-4}$ .



# Posterior distributions for test sample

- As our conditional density estimator is represented by a neural network, we can **directly evaluate the posterior distributions for a given (test) observation.**
- We recover **narrow, well-defined posteriors** for all five parameters that typically contain the ground truth (parameters used for the forward simulation) at the 95% credibility level.



# Posterior distributions for observed population

- With our optimised neural network, we can also **infer the posteriors** for the **pulsar population recorded in our three surveys** and recover the 95% credibility intervals:

$$\mu_B = 13.07^{+0.07}_{-0.08}$$

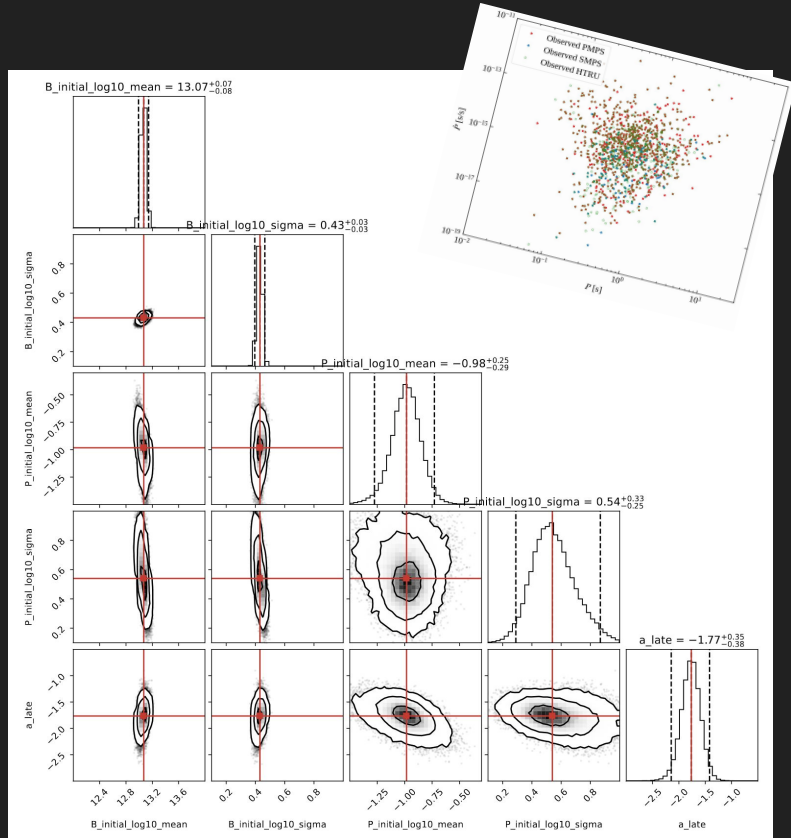
$$\mu_P = -0.98^{+0.25}_{-0.29}$$

$$\sigma_B = 0.43^{+0.03}_{-0.03}$$

$$\sigma_P = 0.54^{+0.33}_{-0.25}$$

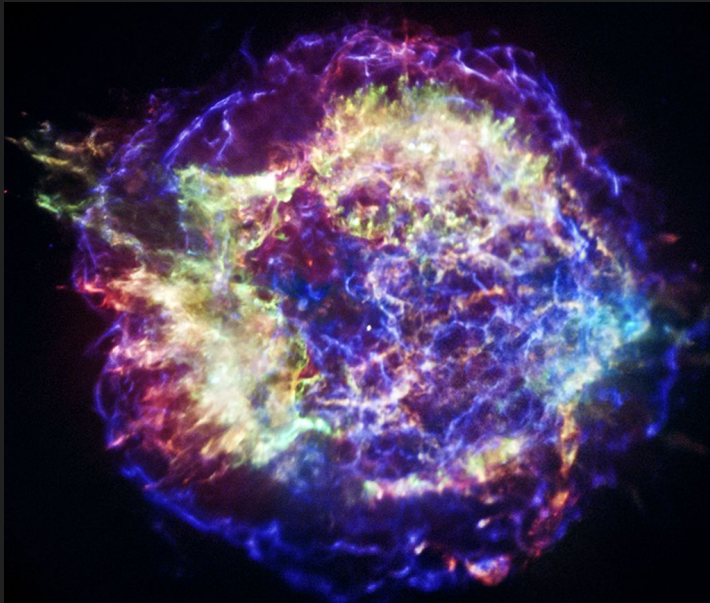
$$\alpha = -1.77^{+0.35}_{-0.38}$$

$$\mathcal{P}(\log P_0) = \frac{1}{\sqrt{2\pi}\sigma_P} \exp\left(-\frac{[\log P_0 - \mu_P]^2}{2\sigma_P^2}\right)$$



# Outline

- **Neutron stars**
- **Pulsar population synthesis**
- **Machine learning and sbi**
- **Inference results**
- **Summary and outlook**



Cassiopeia A supernova remnant  
(credit: NASA/CXC/SAO)

# Take-home points

- Neutron stars are **compact remnants** that **emit pulsed radiation** across the electromagnetic spectrum.
- **Standard radio pulsars** constitutes the largest class of observed neutron star.

- Pulsar **population synthesis** bridges gap between known pulsars and the invisible population.
- It **allows us to constrain birth rates** of different neutron star classes **and birth properties**.

- **Deep learning** with neural networks is ideal to **analyse high-dimensional astrophysical data**.
- **Simulation-based inference** has opened up the possibility for statistical inference **for complex simulators**.

# Outlook

- There are **several directions** that we have started to look into:



# Outlook

- There are **several directions** that we have started to look into:

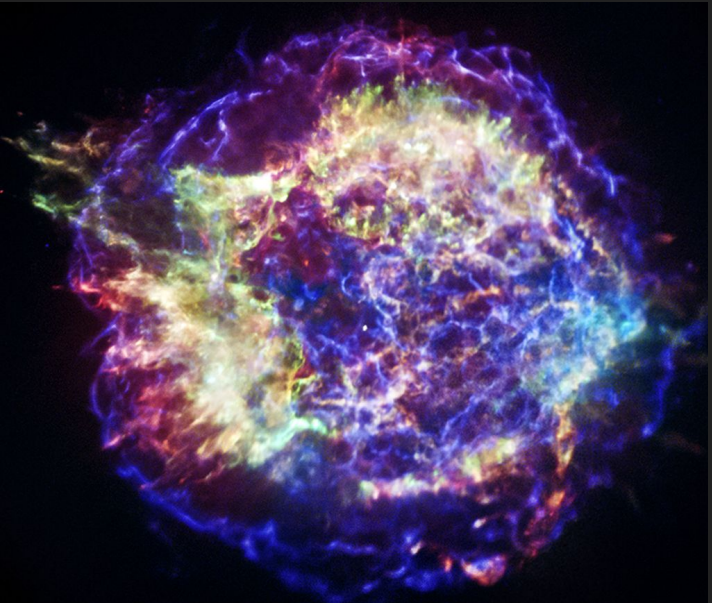
## IMPROVING THE SIMULATOR

- Explore **different assumptions on initial period** and magnetic-field **distributions**
- Extend framework to model also gamma-ray and X-ray emission and **predict the multi-wavelength emission**

## IMPROVING SBI

- **Test other approaches**
- Expand the approach to **active learning** and derive posteriors sequentially **using SNPE**, etc.

# THANK YOU



Cassiopeia A supernova remnant  
(credit: NASA/CXC/SAO)